Supplemental Information

Evidence in biomass burning smoke for a light-absorbing aerosol with properties intermediate between brown and black carbon

Gabriela Adler, Nicholas L. Wagner, Kara D. Lamb, Katherine M. Manfred, Joshua P. Schwarz, Alessandro Franchin, Ann M. Middlebrook, Rebecca A. Washenfelder, Caroline C. Womack, Robert J. Yokelson, Daniel M. Murphy

Is the thermodenuder creating BC and/ intermediate absorber?

The TD was used for the removal of volatile components. It was operated at 250 °C, and included a heated tube with an embedded activated-carbon fabric (CarboCloth™). The heated length was 40 cm followed by a 40 cm unheated section. The active-carbon fabric was embedded along the length of both the heated and unheated sections. The sample flow through the TD was 1.8 slpm. The particle transmission efficiency was measured using atomized and dried NaCl aerosols (NaCl boiling point ~ 800C), the particles were measured using the Laser Aerosol Spectrometer (LAS), to provide the TD transmission as a function of particle size. We found the TD transmission to be 86 ±4% for particles of 100–300 nm at 250 °C. The 4% uncertainty was due to uncertainty in the aerosol source stability and the flow stability when switching between sampling up/downstream of the TD.

We examined the possibility of charring inside the TD, hence creating rBC. We used setup 2 (Figure 1) to examine the rBC mass using the SP2 upstream and downstream of the TD. For all cases, we did not see any evidence that rBC mass increased after the TD. We also used setup 2 to examine the possibility of the intermediate absorber created in the TD, and did not see an increase in the absorption at 661 nm in the TD compared to the bypass, as would be expected if an absorbing material had been created in the TD. However, only one set of size and mass selection data is available.

An additional argument is that fulvic acid aerosol has been found to become more absorbing when subjected to an oven above 500 °C (Sedlacek et al. 2018) and wood tar aerosol changes structure when subjected to 650 °C (Toth et al. 2018). Although this does not definitively prove that there are no changes at 250 °C, the fact that both groups found it necessary to use much higher temperatures makes it unlikely that there are large changes in absorption in a 250 °C thermodenuder.

Retrieval of the mass absorption cross section (MAC) using the CPMA and the SP2

The mass absorption cross section for the SP2 (MAC_{SP2} described below) was determined as the slope of the line-fitting of the absorption (measured by the PAS) as a function of rBC measured by the SP2, calculated for every setting (mass and size selection) averaged for each measurement section (between PAS filter sections). The same method was used for the MAC measured using the CPMA (MAC_{CPMA} described below), where the average mass was obtained using the selected mass multiplied by the number of particles measured by the CPC. A spot check (for 6 fg red absorption in burn 87) showed that using the average absorption during that run along with the average SP2 or CPMA mass gave the same MAC values as the line fits to within a few percent.

Effect of BC coatings on the light absorption for the SEAC4RS fire plume

The PAS measurements were conducted downstream of the TD, for which case a typical assumption is that only a negligible fraction of the coating mass remains (Lack et al. 2012a). A coating remaining on the particles after the TD could enhance the BC absorption (Eabs). At the Fire Lab, BC coatings could be examined after the thermodenuder with the SP2. However, during SEAC4RS, the SP2 did not sample downstream of the TD. Figure S2 shows the results of starting with a core diameter and the coating thickness retrieved using the SP2 upstream of the TD along with the assumption that only 50% of the coating mass was evaporated in the 250ºC TD. Even for this conservative assumption, Figure S1 shows that the absorption enhancement would not be sufficient to account for a factor of three discrepancy between the measured MAC_{SP2} and the literature value. Several cases for refactive index are shown in Figure S1 using core-shell Mie theory with a core-BC refractive index of 1.75+0.8i at 661nm. The shaded light orange area in Figure S1 represents a reasonable range of refractive indices (1.5+0i -1.53+0.02i) for the coating, showing a maximum absorption enhancement (Eabs) <2 for the SEAC4RS measurements. Even a much more absorbing coating (1.7 + 0.08i) does not explain a factor of 3 in absorption. If, as is likely, less than 50% of the coating survived the TD, then the calculated Eabs would be smaller.

AMS mass spectra of morphology-selected particles.

Figure S3 shows a portion of the AMS mass spectra from the morphology-selected experiments shown in Figures 2 and 3, with lodgepole pine canopy fuel at a fixed mass (6 fg), and the 200 nm and 300 nm diameter selections. These spectra are normalized to the total organic mass observed by the AMS. Masses used as tracers for PAHs are highlighted in red, whereas unattributed organic peaks are shown in green. The abundances of ions associated with PAHs (or molecules that fragment to PAHs) are higher in the mass spectra associated with the intermediate absorber (D_m = 200 nm) than the spectra from predominantly BC-containing aerosols (D_m = 300 nm). Both morphologies were downstream of a thermal denuder that should have removed most small PAHs, so these PAHS may have in clusters or adsorbed or otherwise tied to other species.

The default relative ionization (RIE) for organic material (1.4) was used to obtain the estimates of the organic concentrations in Figure S3. The RIE for PAHs is possibly higher than this (Dzepina et al., 2007). Slight adjustments were made for data processing to account for interferences from both organic and sulfate species at the same unit mass resolution peaks in the mass spectra, as described for previous AMS measurements of biomass burning aerosols (Ortega et al. 2013). Because of uncertainties in the collection efficiency and volatilized fraction we emphasize relative ion intensities rather than absolute results.

Dzepina, K., J. Arey, L.C. Marr, D. R. Worsnop, D. Salcedo, Q. Zhang, T. B. Onasch, L. T. Molina, M. J. Molina, and J. L. Jimenez. 2007. Detection of Particle-phase Polycyclic Aromatic Hydrocarbons in Mexico City using an Aerosol Mass Spectrometer. *Int. J. Mass Spectrom.*, 263:152-170.

Ortega, A. M., D. A. Day, M. J. Cubison, W. H. Brune, D. Bon, J. A. De Gouw, and J. L. Jimenez. 2013. Secondary Organic Aerosol Formation and Primary Organic Aerosol Oxidation from Biomass-burning Smoke in a Flow Reactor During FLAME-3. *Atmos. Chem. Phys.,* 13:11551-11571.

Sedlacek III, A. J., T. B. Onasch, L. Nichman, E. R. Lewis, P. Davidovits, A. Freedman and L. Williams. 2018. Formation of Refractory Black Carbon by SP2-induced Charring of Organic Aerosol, *Aerosol Sci. Technol*., 52, 1345-1350, DOI: 10.1080/02786826.2018.1531107.

Tóth, A., A. Hoffer, M. Pósfai, T. Ajtai, Z. Kónya, M. Blazsó, Z. Czégény, G. Kiss, Z. Bozóki, and A. Gelencsér. 2018. Chemical Characterization of Laboratory-Generated Tar Ball Particles, *Atmos. Chem. Phys.*, 18, 10407-10418.

Table S1: The different fuel types and the mass and size selection presented in Figures 2-5

Date	Setup	Fuel	Selected mass (fg)	Selected Mob. Diam (nm)
10/29/2016 Burn 82	1	Excelsior	6 6 6 6 6 6	200 250 275 300 350 375
10/31/2016 Burn 84	2	chaparral (chamise, South Dakota) canopy	6 8 12	250 250 250
11/1/2016 Burn 87	1	lodgepole pine canopy	6 6 6	200 250 300
11/2/2016 Burn 89	2	Ceanothos	6 6 6	250 250 250
11/5/2016 Burn 94-95	2	Chamise (chaparral, New Mexico) canopy	3 3 3	200 150 250
		ponderosa pine, litter	4 4	250 200
11/6/2016 Burn 96	1	longleaf pine Fort Stewart	2 2 3	110 150 175
10/27/2016 Burn 80	3	Douglas-fir	----------	----------
10/26/16 Burn 78	3	Ponderosa Pine	----------	----------
11/2/2016 Burn 88	3	Juniper Canopy	----------	----------
11/1/2016 Burn 86	3	Lodgepole Pine	----------	----------
10/31/2016 Burn 85	3	Sagebrush	----------	----------
Burn 107	3	chaparral (chamise, South Dakota and New Mexico), canopy	---------- -	----------

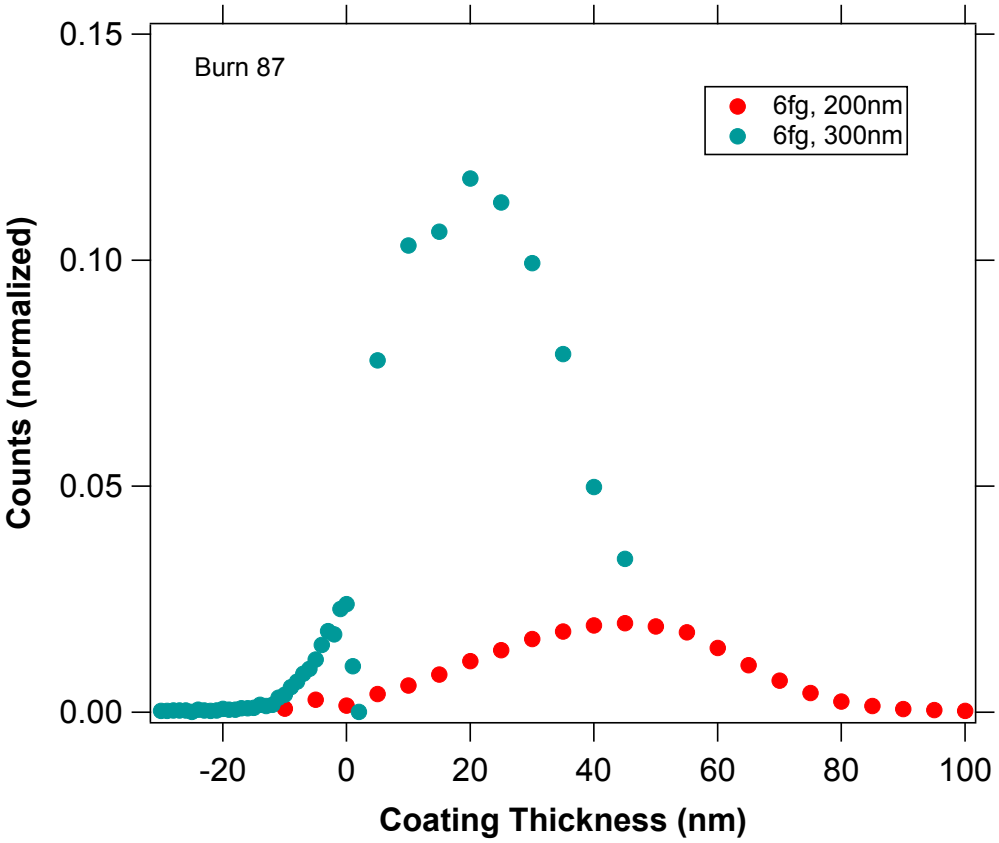

Figure S1: The coating thickness derived from the SP2 for the particles in Figures 2 and 3. The distribution for the 200 nm mobility diameter particles does not add to one because the majority of those (spherical) particles did not include rBC. The uncertainty for a 20 nm coating thickness is significant compared to 20 nm, so it should probably be interpreted as a minimal coating.

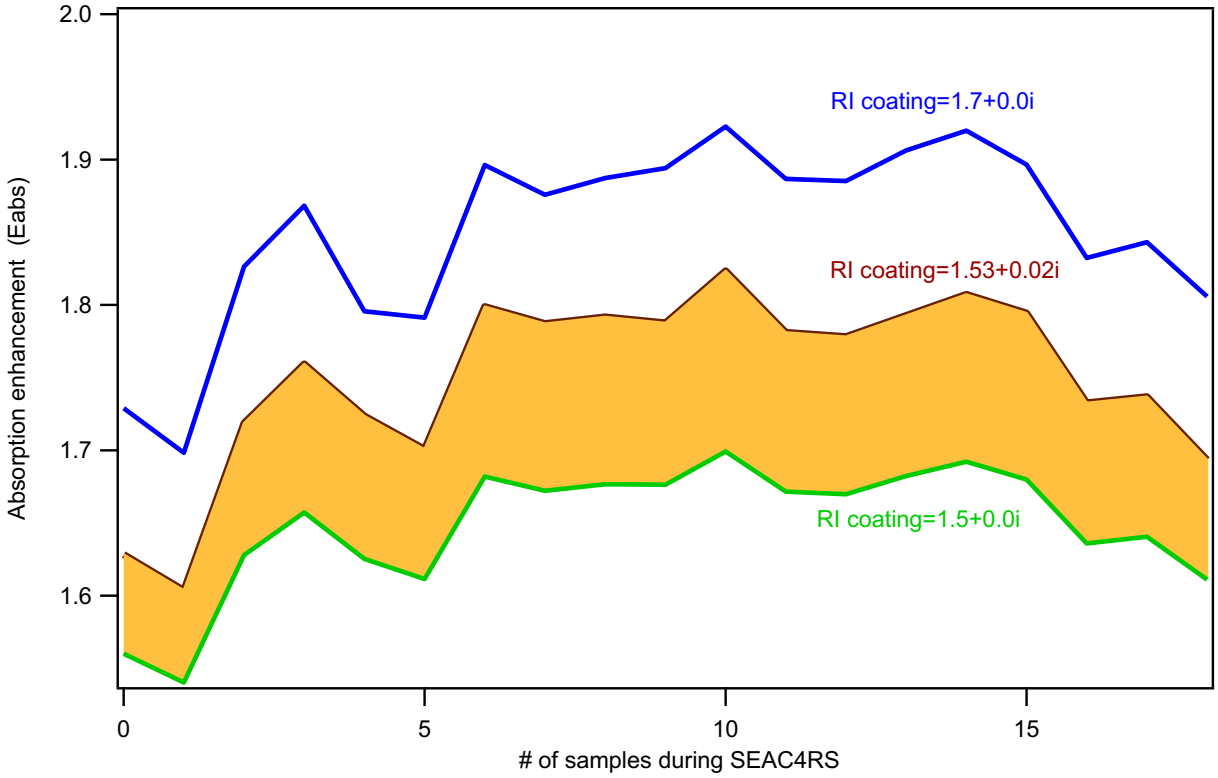

Figure S2: The black carbon absorption enhancement (Eabs) for various refractive indices. The absorption enhancement for all the measured data during the SEAC4RS mission, as a function of the different refractive indices for the organic coating at 660 nm. Assuming spherical particles using Mie theory, the measured core and coating size (by the SP2), and a case where the thermodenuder only removed 50% of the coating thickness. This figure demonstrates that coating is unlikely to account for factor of 3 enhancement between measured and reported MAC values.

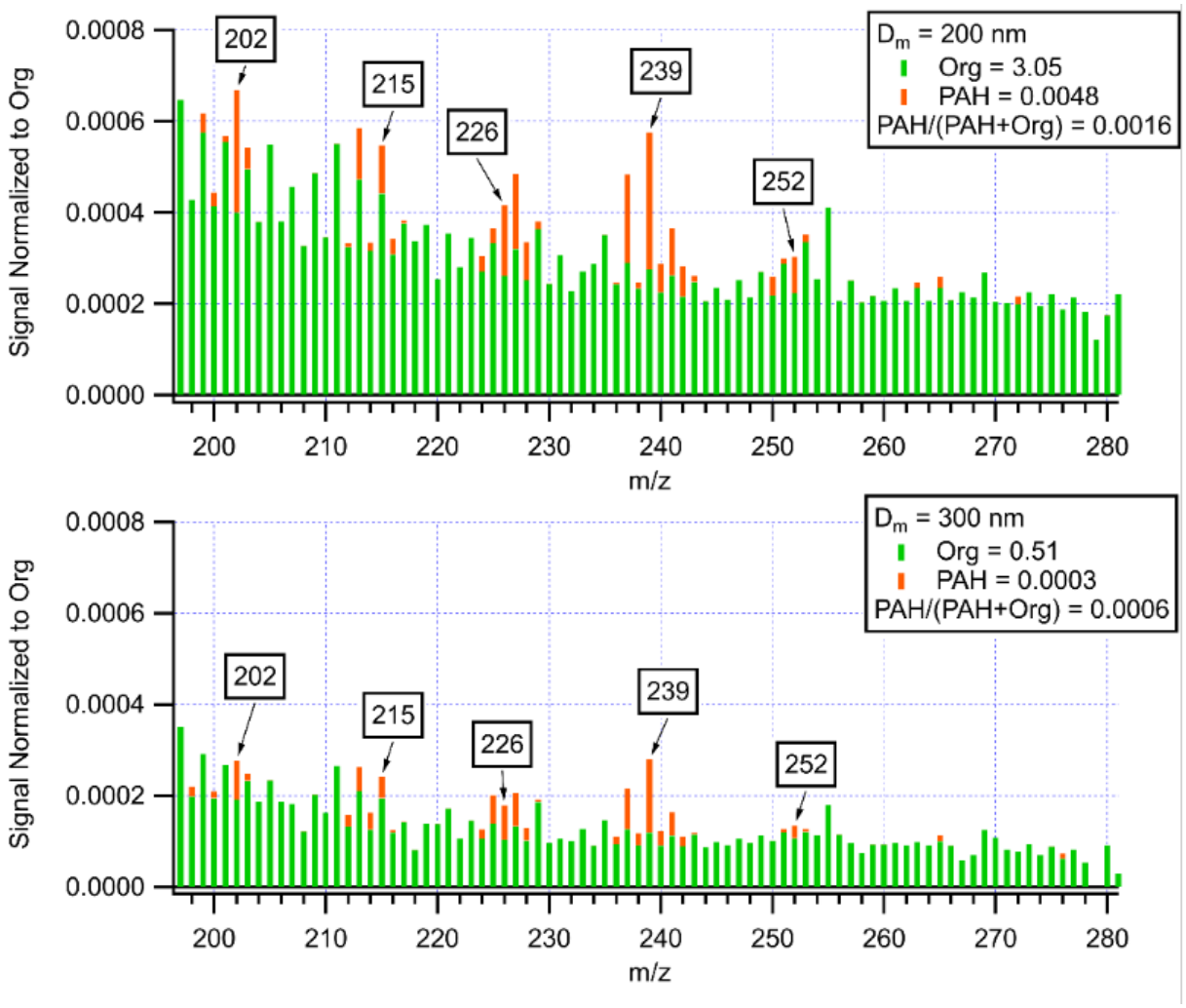

Figure S3: Normalized, average mass spectra of particles during the experiment shown in Figure 3. The AMS default fragmentation pattern for PAHs was used to highlight the peaks characteristic of PAHs (red). Unidentified organic peaks are shown in green. The absolute and relative abundances of PAHs compared to the total organic signal were higher for the particles with the smaller mobility diameter. The 5 peaks identified in both spectra (at m/z 202, 215, 226, 239, and 252) are the same highest peaks observed on average during the rush hour, peak-PAH time period in Mexico City (Dzepina et al. 2007).